

Isak Kloc
Israel Aircraft Industries
Israel

Abstract

Basic concepts of rigid body rolling motion are applied and extended to the treatment of flexible rolling devices operating on rigid surfaces under conditions of slip or skid. A theoretical model is introduced representing the kinematic performance of wheel points located at the deformed contact surface.

Knowing the linear and angular velocities at the wheel axle, governing equations of motion are derived, describing the absolute velocities of points at the contact surface. An expression is developed which provides for the "mean velocity value" at the contact surface, which permits the derivation of the "effective rolling radius" of an elastic device, applicable to aircraft and automotive tires.

Limited experimental evidence indicates that the theory represents approximately the motion performance of elastic rolling devices, particularly tires.

I. Introduction

From a mechanical point of view, wheel axle displacements and rotations are generally initiated and sustained either as a result of applied torques (driven wheels) or towing forces (pulled wheels). These mechanical sources of rolling motion relate to well known rigid wheel velocity regimes namely: slip, roll or skid, each one dependent on the direction or value that the velocity acquires at the point where the wheel contacts the rigid supporting surface.

When considering elastic rolling devices, particularly tires, the lack of a compatible velocity field makes it impossible to define with sufficient accuracy the velocity regimes of skid, roll or slip, as it is normally done for rigid wheels. By definition, a compatible velocity field is one which satisfies the axle's linear and angular velocities V_0 , ω and the kinematic constraints imposed on the contact surface points of the rolling device.

The objective of this study is to determine a compatible velocity field and velocity regime corresponding to an elastic rolling device when the axle velocities V_0 , ω and its deformed configuration are prescribed. To this end a general velocity field is postulated, applicable to elastic rolling devices. Also, a basic equation is derived, which provides for the mean value of the velocity at the contact surface.

Typical tire dynamic problems, where the mean velocity value is of interest, relate to the potential development of tire-ground kinematic friction⁽¹⁾ for purposes of traction, braking or during aircraft landing gear wheel spin-up.

Tire wear and transport efficiency, as dictated by the effective axle displacement per wheel revolution,

are also functions of the velocity regime. In this context, it is of significance to determine the kinematic conditions under which a deformed tire will roll with zero slip. This problem is intimately connected with the definition of the tire effective rolling radius, $R_{e,o}$, a parameter which allows description of the rolling of a (drag force-free) deformed tire by the motion of an equivalent rigid roller of radius $R_{e,o}$. Currently (June 1974), to the writer's knowledge, there is no theoretical formulation or experimental data which defines the kinematic process undergoing at the contact surface of a tire when it rolls with zero slip. Here, the equation of the mean velocity value furnishes, after postulating a zero mean velocity at the tire contact surface, a compatible velocity field and an equation of the effective rolling radius. A semi-empirical expression in the form $R_{e,o} = R - \Delta/3$ (R = tire radius, Δ = tire deflection) based only on tire strains was derived by Whitbread⁽²⁾. Instead, the kinematic solution developed herein, indicates that, in addition to the tire deflection parameter, the $R_{e,o}$ is also controlled by the tire contact length; a fact which may explain the scatter of $R_{e,o}$ measurements⁽³⁾, due to changes in the tire pressure or tire types⁽³⁾.

Results obtained apply only to shallow or circumferentially treaded tires, without considering the effects from cornering forces or high speeds. The theory may also be of interest in the study of landing gear drop tests, mechanical rolling processes connected with land locomotion⁽⁴⁾ and tire hydroplaning phenomena⁽⁵⁾.

As presented, Section II summarises aspects and definitions of the theory of rigid body rolling motion. These concepts are applied in Sections III and IV to study the motion of elastic rolling devices (rollers and tires). First, a kinematic model is postulated and a velocity field derived, for points located at the deformed contact surface. Then the concept of the mean velocity value at the contact surface is introduced and an equation derived permitting estimation of the effective rolling radii of elastic rollers and tires. Finally in Section V, tire rolling experiments and empirical results are compared with the proposed theory.

II. The Motion of Rigid Wheels (Rollers)

Basic concepts of rigid body rolling motion are summarized to be applied later in the study of elastic rolling devices.

Consider a rigid wheel of radius R , rolling with uniform linear velocity V_0 and angular velocity ω . If V_0 and ω are known, the absolute velocity of the wheel axle may be expressed in the form

$$V_0 = \omega R(1+s) = \omega R_I \quad (1)$$

where

$$R_I = R(1+s) \quad (2)$$

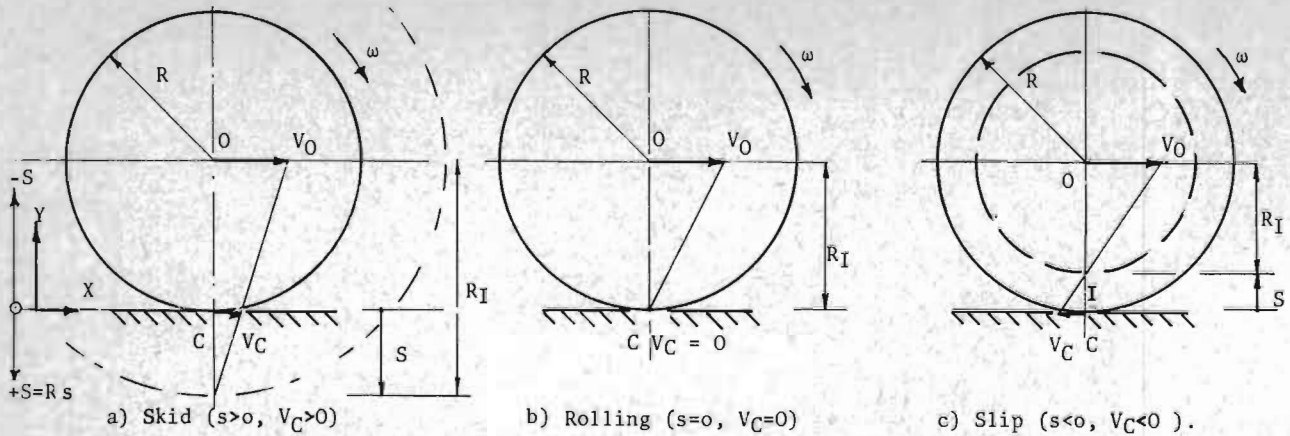


Figure 1. Typical Rolling Regimes of Rigid Rollers

Equation (2) indicates the distance between the center of instantaneous rotation, point I, and the wheel axle, Figure 1.

Given the set of values V_0 and ω , the non-dimensional parameter s is determined from Eq. (1)

$$s = \frac{V_0}{\omega R} - 1; \quad (-1.0 \leq s \leq \infty) \quad (3)$$

The parameter s (3) defines the position of the center of instantaneous rotation with reference to the supporting surface. The sign of s resulting from (3) permits to define the nature of the overall rolling regime. Thus, the wheel either skids, rolls or slips in accordance with $s \geq 0$ respectively as shown in Figure 1. Correspondingly if the direction of the velocity V_C at point C, is the same as V_0 then, the wheel skids. Otherwise, it slips. If $V_C = 0$ it rolls with zero slip.

The above concepts will next be extended to study the kinematics of elastic rollers and tires. The object being, to define the equivalent regimes and velocity characteristics shown in Figure 1 but, applicable to elastic rolling devices.

For simplicity, consider the two dimensional problem of an axially loaded elastic cylinder of radius R , rolling on a rigid surface with uniform linear and angular velocities V_0 and ω , respectively.

The deformed roller configuration is prescribed in terms of the axle height H and footprint contact length $2L$, assumed to be symmetric with reference to the local vertical through the axle O (Figure 2).

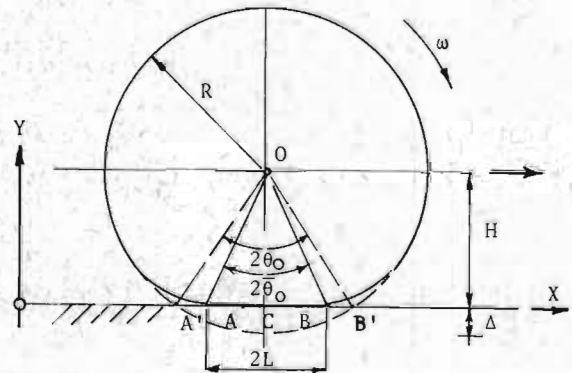


Figure 2. Theoretical and Actual Deformed Roller Configurations.

In general, as a consequence of the mechanical properties of the roller and the mobilized friction stresses at the contact surface interface, the actual footprint length differs from the corresponding theoretically segmented cylinder. This difference is accounted for by means of a contact length parameter k , such as

$$\left. \begin{aligned} 2L &= 2H \tan \bar{\theta}_0 = 2k H \tan \theta_0 \\ k &= \tan \bar{\theta}_0 / \tan \theta_0 \end{aligned} \right\} \quad (4)$$

Where $\bar{\theta}_0$ and θ_0 are the actual and theoretical angles corresponding to the footprint trailing and leading edges, points A, B and A', B', respectively, (For aircraft tires the parameter k is commonly known⁽³⁾, $k \approx 0.85$).

III. Motion of Elastic Rolling Devices

A Kinematic Model of Rolling Motion

The concepts of rigid body rolling motion, laid down in Section II, are concerned with characteristic velocities of skid, roll or slip taking place at a single point, where the roller contacts the surface. If the rolling device deforms elastically, then the kinematic description of the velocity characteristics at the deformed contact surface, is quite complex. In order to study this problem it may be postulated that the deformed roller has two basic regions of motion. One region corresponds to points which lie outside the contact surface and the other, to points lying within the deformed contact surface. The motion of points within each of these two regions may first be described independently using basic kinematic concepts. Once this is accomplished, it is then required to establish the kinematic connection between points located within these two zones.

Once the roller deformed configuration is given as stated above, it is considered that the localized strains do not influence the motion of the contact zone as a whole. Points within this zone are constrained to move along the supporting surface ex-

clusively and their motion may be described with the aid of a kinematic model shown in Figure 3.

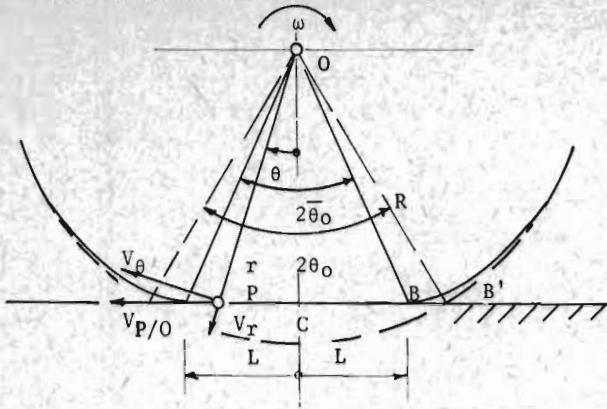


Figure 3. Kinematic Model of Generic Point P

A generic point P, pertaining to the contact surface, is assumed to be represented by a pin constrained to slide along a slot parallel to the surface, while it rotates with angular velocity ω around the axle O. Adopt the moving polar coordinate system (r, θ) , with origin at O. The position of P is defined by the angle θ and the radial vector

$$r = \overline{OP} = \frac{R \cos \theta_0}{\cos \theta}; \quad (\theta \leq \bar{\theta}) \quad (5)$$

The limiting positions of P relate to the angular openings $(\pm \bar{\theta}_0)$ and correspond to the trailing and leading edges of the footprint respectively. The sign of θ is adopted positive if it has the same sign as ω . Based on (5), the radial velocity component along OP is described by

$$V_r = \frac{dr}{dt} = R \frac{\cos \theta_0}{\cos^2 \theta} \sin \theta \frac{d\theta}{dt} \quad (6)$$

where V_r is directed outward, along OP. The transversal velocity component is perpendicular to OP and oriented in accordance with the rotation ω

$$V_\theta = r \frac{d\theta}{dt} = R \frac{\cos \theta_0}{\cos \theta} \frac{d\theta}{dt} \quad (7)$$

From (6) and (7), it is easily seen that $V_r/V_\theta = \tan \theta$, satisfies the motion constraint that the roller contact point P displaces along the surface support. The relative velocity of P with respect to O is determined with (6) and (7), and $\omega = d\theta/dt$

$$V_{P/O} = (V_r^2 + V_\theta^2)^{1/2} = \omega R \frac{\cos \theta_0}{\cos^2 \theta} \quad (8)$$

Equation (8) defines a function symmetric with respect to $\theta = 0$ and continuous for all values of $|\theta| < \bar{\theta}_0$. The points where $\theta = \pm \bar{\theta}_0$ (trailing and leading edges), are subjected to velocity jumps, as strained material enters into and leaves the contact surface. A typical velocity field deduced from Equation (8) for $\bar{\theta}_0 = \pm \pi/6$, is shown in Figure 4.

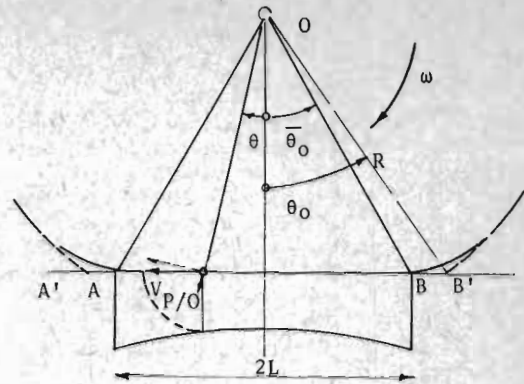


Figure 4. Velocities Relative to Axle O ($\bar{\theta}_0 = \pm \pi/6$)

The absolute velocity of P referred to a fixed (ground) coordinate system XY, obtains from the superposition of the known axle velocity V_0 (positive) and $V_{P/O}$, Equation (8), that

$$V_p = V_0 + V_{P/O} = V_0 - \omega R \frac{\cos \theta_0}{\cos^2 \theta}; \quad (\theta \leq \bar{\theta}_0) \quad (9)$$

The negative sign of $V_{P/O}$ is adopted in connection with V_0 defined as positive.

Equation (9) describes a compatible velocity field corresponding to points at the contact surface of the roller. It indicates that, the contact surface may be subjected to typical velocity fields such as skid, slip, or mixed skid-slip modes, as shown in Figure 5.

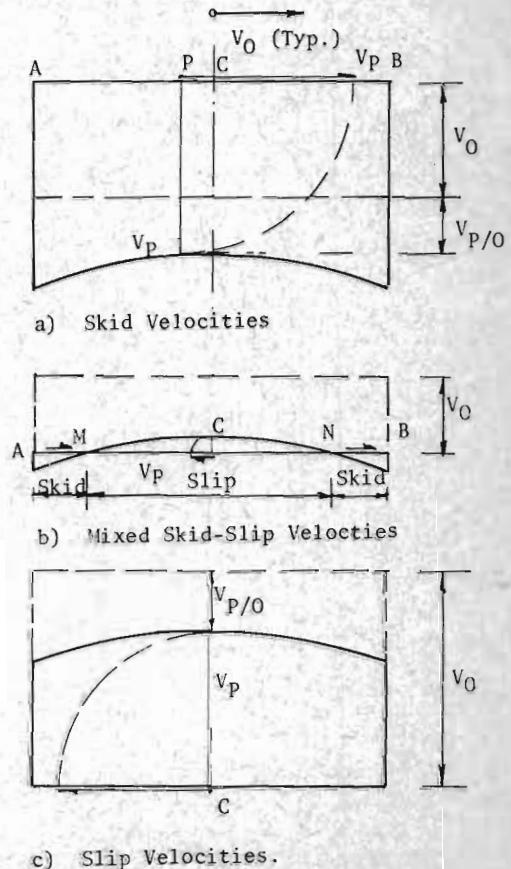


Figure 5. Typical Footprint Velocity Characteristics

The highest skid velocities develop at the contact points B and A, leading and trailing edges, respectively, Figure 5.a). The highest slip velocity occur at $\theta = 0$, point C, Figure 5.c)

The above skid and slip velocity fields represent similar velocity directions to the corresponding velocities of rigid rollers, shown in Figures 1.a) and 1.c) respectively. With regard to the mixed skid-slip velocity field (Figure 5.b), both types of velocity characteristics coexist. Skidding velocities take place at the fore and aft footprint zones (N-B) and (A-M) respectively, accompanied by a central zone (M-N) subjected to slipping velocities. The limiting conditions for the existence of a mixed velocity field are stated in Section IV.

Within the context of velocity regimes, there still remains the problem of specifically defining the kinematic conditions under which an elastic rolling device will operate with zero slip; the equivalent of the rigid roller regime, shown in Figure 1.b). This velocity regime marks the transition between skidding and slipping and represents a basic reference condition. To define this regime, it will prove useful to introduce the concept of the mean velocity value at the contact surface of an elastic rolling device.

The Concept of the Mean Velocity Value

In the following it is postulated that the velocity of the contact surface as a whole be represented by the mean value of the local absolute velocities V_p , Equation (9)*. Since V_0 is constant the value of the mean velocity resultant may also be set in the following form,

$$\bar{V} = (\text{mean } V_p) = V_0 + \bar{V}_{p/0} \quad (10)$$

where $\bar{V}_{p/0}$ represents the mean value of the velocity field $V_{p/0}$, Equation (8). To determine $\bar{V}_{p/0}$ relate an elemental contact length dx with its corresponding $V_{p/0}$, (Figure 6).

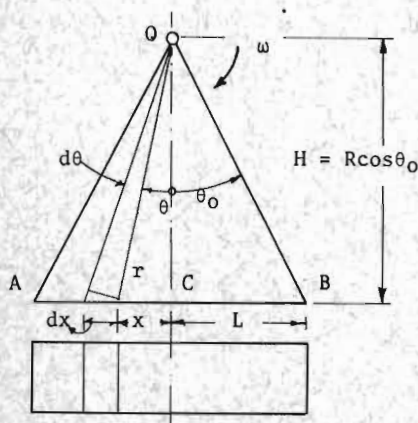


Figure 6. Elastic Roller Footprint Parameters

Thus,

$$V_{p/0} = \frac{2}{L} \int_{x=0}^{x=L} (V_{p/0}) dx \quad (11)$$

* This hypothesis will be tested on the bases of tire effective rolling radius measurements (Section V).

Where $L = kR \sin \theta_0$, and from Figure 6,

$$dx = \frac{R \cos \theta_0}{\cos^2 \theta}$$

After setting the integration limits $\theta = \theta_0$ for $x = L$, and $\theta = 0$ for $x = 0$, (11) reduces to

$$\begin{aligned} \bar{V}_{p/0} &= \frac{\omega R^2 \cos^2 \theta_0}{kR \sin \theta_0} \int_{\theta=0}^{\theta=\theta_0} \frac{d\theta}{\cos^4 \theta} \\ &= -\omega R \cos \theta_0 \left(1 + \frac{k^2}{3} \tan^2 \theta_0\right) \end{aligned} \quad (12)$$

The negative sign of $\bar{V}_{p/0}$ results from V_0 defined as positive.

Consequently, substituting (12) into (10) yields a general equation for the mean value of the absolute velocities at the contact surface of an elastic roller,

$$\bar{V} = V_0 - \omega R \cos \theta_0 \left(1 + \frac{k^2}{3} \tan^2 \theta_0\right) \quad (13)$$

Effective Rolling Radius of Elastic Rollers

By analogy with the motion of rigid wheels (section II), if the axle velocities V_0 , ω and the deformed configuration of the rolling device are given, the corresponding axle velocity may be expressed in the form,

$$V_0 = \omega R (\cos \theta_0 + s) = \omega R_I \quad (14)$$

where s represents a non-dimensional parameter, which defines the position of the center of instantaneous rotation with respect to the surface support as shown in figure 1 and

$$R_I = R (\cos \theta_0 + s) \quad (15)$$

is the distance of the center of instantaneous rotation I from the wheel axle.

Substituting (14) into (13) yields

$$\bar{V} = \omega R \left(s - \frac{1}{3} k^2 \sin \theta_0 \tan \theta_0\right) \quad (16)$$

As an application of Equation (16), it is of interest to determine the condition under which an elastic cylinder rolls with a "zero mean slip" velocity resultant at the contact surface. To postulate that there exists a zero mean slip velocity resultant, means that certain points at the deformed contact surface may be subjected to local differential velocities, but the mean value of the resultant velocity $\bar{V}=0$. This condition is satisfied by Equation (16), when the parameter

$$s = s_0 = \frac{1}{3} k^2 \sin \theta_0 \tan \theta_0 > 0 \quad (\text{see Table 1}) \quad (17)$$

Substituting Equation (17) into Equation (15) yields the effective rolling radius for a zero mean slip velocity condition,

$$R_I = R_{e,o} = R \cos \theta_o \left(1 + \frac{k^2}{3} \tan^2 \theta_o \right) \quad (18)$$

or, in non-dimensional form,

$$R_{e,o}/R = h + \frac{1}{3} \left(\frac{\ell}{h} \right)^2 = f(h, \ell) \quad (19)$$

where the deformation parameter k was defined by (4) with $h=H/R=\cos \theta_o$ and $\ell/h = k \tan \theta_o$, the axle height and contact length parameters respectively (Figure 2) Values of s_o , Equation (17) and of $R_{e,o}/R$ (Equation (19)) are shown in Table 1 as functions of k and θ_o . There are also shown for convenience, the axle height H/R and deflection $\Delta/2R$ parameters. Results indicate that rolling with zero mean slip takes place with an $R_{e,o}/R > h$. For the same roller axle height, R_{eff}/R increases with increasing contact length. Specifically $R_{e,o}/R$ relates to both parameters h and ℓ .

Equation (17) serves also to establish the rolling velocity regimes of elastic rollers, (see Section IV, Equation 30).

IV. The Rolling Motion of Tires

Mean Footprint Tire Velocity

Consider a smooth or circumferentially treaded tire of toroidal cross section with an equatorial radius R . The axle is subjected to the same rolling velocity conditions as defined for the elastic roller in connection with Equation (9).

The mean skid velocity at the tire contact surface is now estimated applying similar concepts as formulated for the elastic roller, Equation (10); the only difference being that the shape of the tire imprint approximates an ellipse², Figure 7.

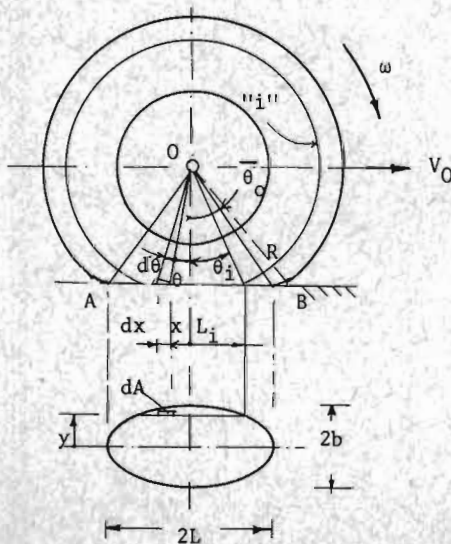


Figure 7 - Tire Footprint Parameters

The mean value $\bar{V}_{P/O}$ of the tire contact surface velocity, relative to the axle O , for a given elliptical footprint area A , is defined by

$$\bar{V}_{P/O} = \frac{1}{A} \int_A V_{P/O} dA \quad (20)$$

Where $V_{P/O}$, defined by Equation (8), applies to an elemental area $dA = dx dy$ within the tire imprint region. The elemental contact length dx , corresponds to a generic circumference "i" at a distance y from the tire equatorial (mean) plane (Figure 7,) is defined by

$$dx = \frac{R \cos \theta_o}{\cos^2 \theta} d\theta \quad (21)$$

Substituting (8) and (21) into (20), yields,

$$\bar{V}_{P/O} = \frac{4\omega R^2 \cos^2 \theta_o}{A} \int_{y=0}^{y=b} dy \int_{\theta=0}^{\theta=\theta_i} \frac{d\theta}{\cos^4 \theta} \quad (22)$$

The integration limits in (22), are deduced noting that, $\theta = \theta_i$ represents the central angle of the half contact length L_i corresponding to the circumference "i", Figure 7. Points on the periphery of the ellipse with major and minor semi-axes L and b , are defined by

$$\left(\frac{L_i}{L} \right)^2 + \left(\frac{y}{b} \right)^2 = 1$$

from which the integration limit (22) reduces to

$$\bar{\theta}_i = \tan^{-1} \left(\frac{L_i}{H} \right) = \tan^{-1} \left(\frac{L}{b} \frac{(b^2 - y^2)^{1/2}}{H} \right) \quad (23)$$

Integrating (22) and substituting for the corresponding limits (23), noting that the ellipse area $A = \pi L b$; the mean value of the slip velocity, relative to the axle O , reduces to

$$\bar{V}_{P/O} = -\omega R \cos \theta_o \left(1 + \frac{k^2}{4} \tan^2 \theta_o \right) \quad (24)$$

where the negative sign of (24) results from V_0 defined as positive. Substituting (24) into (10), yields a general equation for the mean value of the absolute velocities at the contact surface of a tire,

$$\bar{V} = V_0 - \omega R \cos \theta_o \left(1 + \frac{k^2}{4} \tan^2 \theta_o \right) \quad (25)$$

Substituting (15) into Equation (25) yields

$$\bar{V} = \omega R \left(s - \frac{k^2}{4} \sin \theta_o \tan \theta_o \right) \quad (26)$$

A comparison of Equation (16) and (26), shows the close analogy between the rolling motion of elastic cylinders and tires in terms of the mean value that the absolute velocities acquire at their respective contact surfaces.

Effective Rolling Radius of Tires

As an application of Equation (26) it is of interest to determine the conditions under which a tire will roll with a "zero mean slip" velocity resultant at the contact surface. From Equation (26) setting $\bar{V} = 0$,

$$s = s_o = \frac{k^2}{4} \sin\theta_o \tan\theta_o > 0 \tag{27}$$

A result which indicates that a tire rolls with zero mean slip when its center of instantaneous rotation is located at a distance $S_o = R s_o$, below the surface support.

Equation (27) serves also to establish the tire rolling velocity regime by using Equation (30)

With the help of Equation (27) it, is now possible to deduce the corresponding tire effective rolling radius $R_I = R_{e,o}$ at a zero mean slip. From Equation (16) and (25),

$$R_{e,o} = R \cos\theta_o (1 + \frac{k^2}{4} \tan^2\theta_o) \tag{28}$$

or in non-dimensional form

$$R_{e,o} / R = h + \frac{1}{4} (\frac{\ell}{h})^2 = F(h, \ell) \tag{29}$$

where k, h and ℓ have been defined in connection with (4) and (19).

Values of s_o (Eq.27) and $R_{e,o}/R$ (Eq.29) are given in Table 1 and conveniently shown, either as functions of θ_o , H/R or $\Delta/2R$. Always $R_{o,e}/R > h$.

For the same axle height, the tire inflation pressure will influence the $R_{e,o}$ to the extent that it affects the contact length parameter ℓ . The $R_{e,o}$ is related to both h and ℓ , this fact may explain why tire measurements of $R_{e,o}$ appear to produce an apparent scatter, when results are evaluated on the bases of tire deflections only. This aspect will be considered in the next Section. A comparison of Equations(19) and (29) shows the close analogy between the motion of elastic rollers and tires, in terms of their effective rolling radii.

Mean Velocity Regimes

Having defined the mean zero slip velocity, it is now possible to specifically determine the operating mean velocity regimes of elastic rolling devices, including tires. In effect, given the axle velocities V_o , ω and deformation parameters (4); from Equation (14), the position of the center of instantaneous rotation is related to

$$s = \frac{V_o}{\omega R} - \cos\theta_o \tag{30}$$

Now, in complete analogy to the motion of rigid rollers (Figure 1), comparing s from equation (30) with s_o , from Equations (17) or (27), there results: if $s > s_o$, the contact surface is subjected to a mean skid velocity; if $s < 0$ there is a mean slip velocity and if $s = s_o$ rolling takes place with zero mean slip.

Limiting conditions for the existence of a mixed velocity field of the type shown in Figure 5b, are defined by (9), when $V_p = 0$, and occur for an operating range of $V_o/\omega R$ values, such that

$$\cos\theta_o < \frac{V_o}{\omega R} < 1/\cos\theta_o$$

The mean absolute velocity value at the contact surface of elastic rollers and tires were given by (13) and (25) respectively. Both equations may also be set in the form,

$$\bar{V} = V_o - \omega R_e$$

where

$$R_e = R \cos\theta_o (1 + \frac{k^2}{n} \tan^2\theta_o) = R_{e/o} \tag{31}$$

Equation (31) represents the equivalent rolling radius of the device with $n = 3$, for elastic rollers and $n = 4$, for tires.

In summary, the motion of an elastic rolling device can also be studied on the bases of the motion of an ideal rigid roller of radius R_e given by Equation (31) and corresponding velocity characteristics \bar{V} given by Equations (16) or (26). The mean velocity \bar{V} applies at a vertical distance R_e , below the axle, as shown in Figure 8.

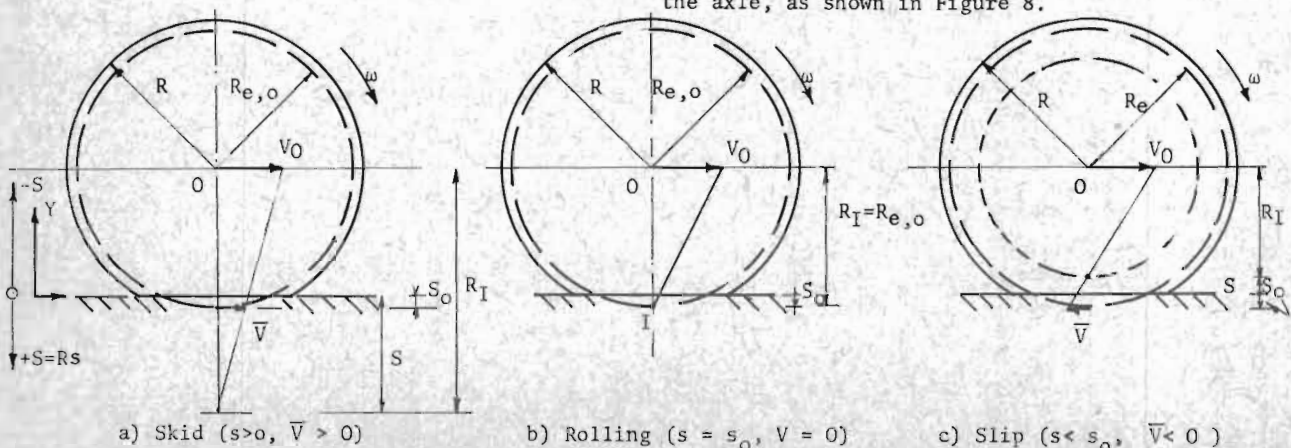


Figure 8. Typical Velocity Regimes of Elastic Rolling Devices. (Tires)

TABLE 1 : EFFECTIVE ROLLING RADIUS PARAMETER ($R_{e,o}/R$)

- ELASTIC ROLLERS AND TIRES -

	TETAZ (RAD)	H/R	DELTA/2R	SZERO		$R_{e,o}/R$		
				ROLLERS	TIRES	ROLLERS	TIRES	
				Eq. (17)	Eq. (27)		EMPIRICAL	THEORETICAL
K= .85	.00	1.0000	.0000	.0000	.0000	1.0000	1.0000	1.0000
	.10	.9950	.0025	.0024	.0018	.9974	.9983	.9968
	.20	.9801	.0100	.0097	.0073	.9898	.9934	.9873
	.30	.9553	.0223	.0220	.0165	.9774	.9851	.9718
	.40	.9211	.0395	.0397	.0297	.9607	.9737	.9508
	.50	.8776	.0612	.0631	.0473	.9407	.9592	.9249
	.60	.8253	.0873	.0930	.0698	.9184	.9418	.8951
	.70	.7648	.1176	.1307	.0980	.8955	.9216	.8629
	.80	.6967	.1516	.1779	.1334	.8746	.8989	.8301
	.90	.6216	.1892	.2377	.1783	.8593	.8739	.7999
K= .90	.00	1.0000	.0000	.0000	.0000	1.0000	1.0000	1.0000
	.10	.9950	.0025	.0027	.0020	.9977	.9983	.9970
	.20	.9801	.0100	.0109	.0082	.9909	.9934	.9882
	.30	.9553	.0223	.0247	.0185	.9800	.9851	.9738
	.40	.9211	.0395	.0445	.0333	.9655	.9737	.9544
	.50	.8776	.0612	.0707	.0530	.9483	.9592	.9306
	.60	.8253	.0873	.1043	.0782	.9296	.9418	.9036
	.70	.7648	.1176	.1465	.1099	.9113	.9216	.8747
	.80	.6967	.1516	.1994	.1496	.8961	.8989	.8463
	.90	.6216	.1892	.2665	.1999	.8881	.8739	.8215
K=1.00	.00	1.0000	.0000	.0000	.0000	1.0000	1.0000	1.0000
	.10	.9950	.0025	.0033	.0025	.9983	.9983	.9975
	.20	.9801	.0100	.0134	.0101	.9935	.9934	.9901
	.30	.9553	.0223	.0305	.0229	.9858	.9851	.9782
	.40	.9211	.0395	.0549	.0412	.9759	.9737	.9622
	.50	.8776	.0612	.0873	.0655	.9649	.9592	.9431
	.60	.8253	.0873	.1288	.0966	.9541	.9418	.9219
	.70	.7648	.1176	.1809	.1357	.9457	.9216	.9005
	.80	.6967	.1516	.2462	.1847	.9429	.8989	.8814
	.90	.6216	.1892	.3290	.2468	.9506	.8739	.8684

V. Tire Rolling Measurements

It is of interest to verify if the postulated velocity field, Equation (8), and the concept of the mean value of the velocity at the tire contact surface, Eq. (26), are representative of expected tire rolling performance.

Since the tire effective rolling radius $R_{e,o}$, Eq. (28), was derived on the bases of the afore mentioned kinematic conditions, rolling test measurements of $R_{e,o}$ will next be used to verify the theory.

Measurements of $R_{e,o}$ for various types of aircraft tires and corresponding footprint-length are given in Reference 3. Three sets of aircraft tires are selected for analysis as shown in Table 2, where the results of rolling test measurements of $R_{e,o}$ are presented in terms of the deflection $\Delta/2R$ and footprint length k (Eq. 4) parameters. Corresponding values of k have been scaled from Fig. 3 of Ref. 3 as applicable to the tires under consideration.

It is noted that the parameter k is not a constant and on the average it approximates the value $k=0.85$, being a function of the type of tire, loading conditions and mobilized friction at the contact surface interface.

Table 2 - Effective Rolling Radius ($R_{e,o}/R$)

Tire Type	$\Delta/2R$	k	Test Ref. (3)	Empirical Ref. (2)	Theory	
					Roller Eq. (19)	Tire Eq. (29)
40 x *	.053	.834	.940	.965	.946	.931
	.074	.825	.921	.950	.924	.906
	.130	.836	.897	.913	.883	.868
26 x **	.073	.896	.948	.951	.939	.918
	.082	.900	.949	.945	.933	.910
	.089	.900	.942	.941	.928	.902
	.135	.840	.917	.910	.882	.844
57 x †	.063	.858	.958	.958	.940	.922

* 40 x 12 - 14PR - VII - R24-B

** 26 x 6.6 -12PR - VII - R23-B

† 57 x 20 - 16Ply- I(56-inch)-R54.

The measurements of $R_{e,0}$ are contrasted with the semi-empirical⁽²⁾ equation and the theoretical results for elastic rollers and tires. This limited analysis indicates that the elastic roller Eq. (19) approximates better the $R_{e,0}$ measurements than the tire Eq. (29).

This fact may be explained on the bases that $R_{e,0}/R$, (Eq. 29) relates to k^2 scaled from a graph of L/R vs $\Delta/2R$ ⁽³⁾ and also because Equation (29) was derived neglecting the influence of tire strains.

Further measurements of $R_{e,0}$ ⁽³⁾ for similar tire types and varying inflation pressures p , indicate that, for the same tire deflection parameter $\Delta/2R$, the $R_{e,0}$ increases with increasing p . This would be confirmed by Equations (19) and (29) only if in order to maintain the same tire deflection Δ an increase of axle load becomes associated with a larger footprint length. Obviously the influence of tire pressure and footprint length on the effective rolling radius cannot be explained by the semi-empirical expression of $R_{e,0}$ since the latter only depends on the deflection Δ .

In general, the values and trends of $R_{e,0}$ Eq. (19), defined for an elastic roller, are considered to be also applicable to tires. Finally, the rather close approximation obtained for $R_{e,0}$ appears to indicate that the velocity field, defined by Eq. (8) is representative of expected tire motion performance.

Conclusions

An admissible velocity field corresponding to points at the contact surface of rolling elastic devices, was postulated. Its application to elastic rollers and tires, indicates that the contact area may be subjected to either one of the following velocity fields: skid, slip and mixed skid-slip modes. These velocity fields may be estimated in detail if the axle velocities and deformed configuration of the device are prescribed.

The kinematic model adopted indicates that maximum skid velocities occur at the leading and trailing edges of the contact surface. Instead, maximum slip velocities take place at the center of the contact area.

The operating range of axle velocities $V_0/\omega R$ for the existence of a mixed skid-slip velocity field has also been defined.

The mean value of the velocity at the contact surface permits to define the wheel operating regime. In particular a zero mean slip velocity condition is introduced, applicable to elastic rolling bodies, particularly tires. This development permits to calculate the effective rolling radius $R_{e,0}$ corresponding to a (drag force-free) tire, confirming the fact that, $R_{e,0}$ is larger than the axle height. It further indicates that, in addition to the tire deflection parameter the $R_{e,0}$ is also controlled by the tire contact length, which may explain the influence of tire pressure on the value of the effective rolling radius.

A comparison of the theory with limited test measurements, indicates that the elastic roller equation represents a close approximation to the kinematic performance of a tire. Results apply to smooth or circumferentially treaded tires.

Acknowledgments

The writer wishes to acknowledge his appreciation for the help received from Mr. M. Fuchs in preparing the computer program.

Nomenclature

A	Footprint area
b	Width of footprint
H	Axle height
$h=H/R$	Axle height parameter
k	Contact length parameter
L	Footprint half-length
$\ell=L/R$	Contact length parameter(footprint).
R	Radius of a rigid or elastic roller. Radius of tire equator.
R_I	Distance of center of instantaneous rotation to wheel axle.
R_e	Equivalent radius of an elastic roller or tire
$R_{e,0}$	Effective rolling radius at zero slip
r	Radial distance
$s = S/R$	Parameter of center of instantaneous rotation
V_0, \bar{V}	Linear and Mean Velocities.
ω	Wheel angular velocity, radians/sec
θ	Angle, wheel rotation
Δ	Vertical deflection
$\delta = \Delta/2R$	Deflection parameter.

References

1. H. Tomita. "Tire-Pavement Friction Coefficients" Naval Civil Engineering Lab. Port Hueneme, California, TR-R 672 (AD 705 987), April 1970.
2. R. Hadekel. "The Mechanical Characteristics of Pneumatic Tyres" - A Digest of Present Knowledge S & T Memmo. No. 5/52, British Ministry of Supply, TPA3/TIB, November, 1952.
3. R.F. Smiley and W.B. Horne. Mechanical Properties of Pneumatic Tires with Special Reference to Modern Aircraft tires. Langley Research Center, Langley Field, Va. TR-R-64, 1960.
4. I. Kloc. "Mechanical Interaction of a Driven Roller (Wheel) on Soil Slopes". Jet Propulsion Laboratory, TM 33-477, June 15, 1971.
5. W.B. Horne and R.C. Dreher: Phenomena of Pneumatic Tire Hydroplaning". NASA TN D-2056, November 1963.